Layered Mixed Transition Metal Oxide Cathodes with Reduced Cobalt Content for Lithium Ion Batteries

Jie Xiao, Natasha A. Chernova, and M. Stanley Whittingham*

Chemistry and Materials, State University of New York at Binghamton, Binghamton, New York 13902-6000

Received August 28, 2008. Revised Manuscript Received October 10, 2008

The structural and physical properties of the low cobalt material, $LiNi_{0.45}Mn_{0.45}Co_{0.1}O_2$, have been investigated. Nearly stoichiometric $LiNi_{0.45}Mn_{0.45}Co_{0.1}O_2$ with the optimal electrochemical performance was produced at 800 °C by coprecipitation method. A higher synthesis temperature leads to a higher crystallinity and larger particles not influencing the Ni/Li disorder. Nonstoichiometric $Li_{1+z}(Ni_{0.45}Mn_{0.45}Co_{0.1})_{1-z}O_2$, $0.8 \leq 1 + z \leq 1.2$, were then studied; it was found that the interslab Ni content increases as the lithium content decreases. However, the lithium content in the metal layer decreases simultaneously minimizing the formation of tetrahedral lithium upon charging. As a result, the Li-deficient $Li_{0.9}(Ni_{0.45}Mn_{0.45}Co_{0.1})_{1.1}O_2$ has the best electrochemical capacity (190 mAh/g between 2.5 and 4.6 V at 0.5 mA/cm^2) and cycleability. The electrochemical performance is compared to that of other well-studied $Li(Ni_yMn_yCo_{1-2y})O_2$ materials with $y = 1/3$, 0.4, 0.425, and 0.5. The magnetism of $Li_{1+z}(Ni_{0.45}Mn_{0.45}Co_{0.1})_{1-z}O_2$ studied in conjunction with the structure is dominated by the ordering of interlayer and intralayer ferrimagnetic clusters. The interlayer clusters nucleate at interslab Ni^{2+} ions and their size increases with the Ni/Li disorder, while the intralayer clusters size increases in materials with larger particle size and smaller amount nonmagnetic ions in the transition metal layers. This model allows using magnetism to estimate the character of the transition metal ordering.

Introduction

Layered inorganic materials have provided most of the cathodes for lithium batteries. In 1980, Mitzushima et al. showed[1] that $LiCoO_2$ was very reversible and had a high potential, allowing it to be used with a carbon based anode. However, its energy storage capability was no higher than that of $LiTiS_2$ because only 50% of the lithium could be cycled without structural instabilities occurring. Although the $LiC_6/LiCoO_2$ system dominates the battery market for small systems such as cell phones and computers, the cost and scarcity of cobalt precludes its use for large-scale applications such as electric vehicles. The isostructural $LiNiO_2$ and $LiMnO_2$ are not suitable substitutes because on lithium removal the former can release oxygen raising major safety issues and the latter converts to the spinel, $LiMn_2O_4$ with irreversible loss of capacity.

Recently, the mixed metal oxides such as $LiNi_{0.33}Mn_{0.33}Co_{0.33}O_2$[2,3] have found favor because of their much better stability, and may now be found in commercial cells. Each element in this mixture plays a significant role. The nickel is the electrochemically active specie, with its oxidation state reversing between 2+ and 4+; the manganese provides stability to the structure and remains in the 4+ oxidation state throughout electrochemical cycling; and the cobalt helps in ordering the lithium and nickel ions, as in its absence around 10% of the nickel and lithium ion-exchange sites.[4] A further complication with this system is that the lithium content can be increased beyond unity, such as in $Li_{1+z}(Ni_{0.33}Mn_{0.33}Co_{0.33})_{1-z}O_2$, all the way to Li_2MnO_3.

Although the $LiNi_{0.33}Mn_{0.33}Co_{0.33}O_2$ composition (known as 333) has been commercialized, there appears to be no obvious reason why this particular composition was chosen. We earlier showed that the $LiNi_{0.4}Mn_{0.4}Co_{0.2}O_2$ (442) material behaved just as well as the 333 material.[5,6] There is therefore a need to determine (a) what is the best mix of nickel, manganese, and cobalt for a long-lived high-power and high-energy-density lithium battery, (b) whether excess lithium improves the electrochemical characteristics, and (c) whether it is beneficial to incorporate other elements into the structure such as fluorine to increase the cell potential or inert elements such as aluminum, as in $LiNi_{0.95-y}Co_yAl_{0.05}O_2$ to increase the stability. Recently, Doeff et al. reported[7] the positive influence of replacing one-quarter of the cobalt in the 442 compound by aluminum, $LiNi_{0.4}Mn_{0.4}Co_{0.15}Al_{0.05}O_2$. To make these determinations, one must gain a better understanding of the overall system. The effect of composition and synthesis conditions on product morphology, stoichiometry and transition metal (TM) ordering need to be understood. Moreover,

* Corresponding author. Tel.: (607) 777-4623, Fax: (607) 777-4623. E-mail: stanwhit@gmail.com.

(1) Mitzushima, K.; Jones, P. C.; Wiseman, P. J.; Goodenough, J. B. *Mater. Res. Bull.* **1980**, *15*, 783.
(2) Ohzuku, T.; Makimura, Y. *Chem. Lett.* **2001**, 642.
(3) Lu, Z.; MacNeil, D. D.; Dahn, J. R. *Electrochem. Solid-State Letters* **2001**, *4*, A200.
(4) Whittingham, M. S. *Chem. Rev.* **2004**, *104*, 4271.
(5) Ngala, J. K.; Chernova, N. A.; Ma, M.; Mamak, M.; Zavalij, P. Y.; Whittingham, M. S. *J. Mater. Chem.* **2004**, *14*, 214.
(6) Ma, M.; Chernova, N. A.; Toby, B. H.; Zavalij, P. Y.; Whittingham, M. S. *J. Power Sources* **2007**, *165*, 517.
(7) Doeff, M. M. *DOE Office of Vehical Technologies Annual Review Meeting*, Bethesda, MD, Feb 25−29, 2008; Department of Energy: Washington, D.C., 2008.

10.1021/cm802316d CCC: $40.75
Published on Web 11/19/2008

cations in addition to the lithium ions migrate during cycling so the material must be considered as a living system. Much of the published work has been reviewed and will not be repeated here.[4,8]

In this paper, we report on a study in which we further reduce the cobalt fraction to just 10% of the transition metal content in $LiNi_{0.45}Mn_{0.45}Co_{0.1}O_2$ (992 compound), in order to understand the impact of such a low cobalt content on the structure and metal ordering using diffraction and magnetic measurements, building on our recent magnetic study.[9] We have synthesized this composition both with a 1:1 Li to transition metal ratio and with lithium excess and deficiency $Li_{1+z}(Ni_{0.45}Mn_{0.45}Co_{0.1})_{1-z}O_2$, characterized the compounds structurally, determined their electrochemical properties, and compared these to the 442 and other compositions.

Experimental Section

$LiNi_{0.45}Mn_{0.45}Co_{0.1}O_2$ was synthesized from $Ni_{0.45}Mn_{0.45}Co_{0.1}(OH)_2$ coprecipitate.[5] Stoichiometric amounts of the soluble salts, $Mn(OAc)_2 \cdot 4H_2O$, $Co(OAc)_2 \cdot 4H_2O$, and $Ni(OAc)_2 \cdot 4H_2O$ were dissolved in deionized water. An excess amount of LiOH solution ($LiOH \cdot H_2O$, ACS, 98%, Alfa Aesar) was added to precipitate the mixed hydroxide; the solid was then thoroughly washed twice with deionized water to remove residual Li salts. The coprecipitate of nickel, manganese and cobalt hydroxides was dried at 65 °C overnight and then mixed with the appropriate amount of $LiOH \cdot H_2O$ to give different Li/(Ni+Mn+Co) molar ratios. A 5% excess of lithium was added to compensate for the evaporation of lithium at high temperatures. The well-ground powders were pressed into pellets and heated first at 450 °C for 12 h and then reground and pressed again. After being further heated at various temperatures from 700 to 1000 °C for another 8 h, the final products were cooled slowly into room temperature. For comparison, another sample of the same composition was quenched after each heating by taking the pellet out of the oven and sandwiching it between two cold copper plates.

X-ray diffraction (XRD) data was collected from 10 to 90° 2θ at a rate of 0.5°/min at room temperature on a Scintag XDS2000 $\theta - \theta$ diffractometer equipped with a Ge(Li) solid state detector. Chemical analysis of the samples was done by direct current plasma spectroscopy (DCP, ARL Fisons SS-7). The specific surface areas were determined by the single-point Brunauer, Emmett, and Teller method (BET, Micromeritics, ASAP2020, Surface Area and Porosity Analyzer). The morphology of $Li(Ni_{0.45}Mn_{0.45}Co_{0.1})O_2$ was examined using a Transmission Electron Microscope (TEM, Hitachi S-570, Japan). A SQUID magnetometer (Quantum Design MPMS XL-5) was used to measure the dc magnetic susceptibility ($\chi = M/H$, M is magnetization, H is applied magnetic field) of the samples from 400 to 2 K in a magnetic field of 1000 Oe. Field-cooled (FC) and zero-field-cooled (ZFC) magnetizations were measured from 298 to 2 K in the magnetic fields of 10 Oe. FC susceptibility was measured by cooling the sample in the magnetic field; before taking ZFC data, the remanent magnetic field was quenched to less than 3 mOe, the sample was cooled to 2 K, and the magnetic field was then applied and the temperature dependence was measured while heating the sample. Magnetization curves were measured at 5 K in magnetic fields up to 5 T. The sample was zero-field-cooled to 5 K before the magnetization data was taken. Electrochemical properties were tested in 2325-type coin cells on a VMP2 multichannel potentiostat (Biologic). The cathode was constructed by mixing the oxide with acetylene black and poly(vinylidene fluoride) (PVDF) powder in a weight ratio of 80:10:10. The loading of each cathode was usually around 20 mg/cm^2. Pure lithium foil (Aldrich, thickness 0.38 mm) was used as a counter and reference electrode. The electrolyte used was 1 M $LiPF_6$ (lithium hexafluorophosphate) in a mixture of DMC (dimethyl carbonate) and EC (ethylene carbonate) with 1:1 volume ratio (LP30 from EM Industries). The assembly of the coin cells was performed in a helium-filled glovebox. The coin cells were cycled within chosen voltages at a current density of 0.5 or 0.1 mA/cm^2 at room temperature.

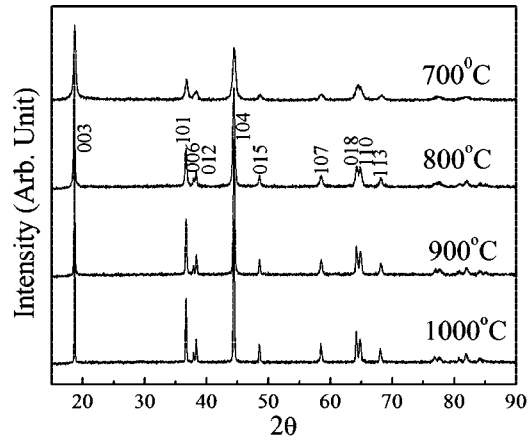

Figure 1. X-ray diffraction patterns for $Li(Ni_{0.45}Mn_{0.45}Co_{0.1})O_2$ synthesized at 700, 800, 900, and 1000 °C showing increasing crystallinity with higher temperature. The hexagonal Miller indices are shown.

Results and Discussion

The XRD patterns of the $LiNi_{0.45}Mn_{0.45}Co_{0.1}O_2$ compounds synthesized at 700, 800, 900, and 1000 °C are shown in Figure 1 with the hexagonal Miller indexes indicated. The samples are all single phases, with the α-$NaFeO_2$ type structure (space group $R\bar{3}m$). When the synthesis temperature increases, the intensities of all the peaks also increase and the peaks become sharper reflecting the increasing particle size and crystallinity. The splitting of the hexagonal 018 and 110 peaks at around 64°, often used as an indication of layered structure, becomes better defined as the temperature increases from 700 to 1000 °C, suggesting that the layered structure is getting more complete at higher temperatures.

Ma et al. used powder neutron diffraction to show that only Ni^{2+} in the transition metal layers exchanges sites with Li^+ ions between the layers.[6] Therefore we only consider the nickel and lithium disorder between the 3a and 3b sites in the Rietveld refinement of the X-ray diffraction data using the GSAS/EXPGUI package.[10] In the refinement procedure, the occupation factors of Mn and Co were set to be 0.45 and 0.1, respectively. The results of the refinement (Table 1) indicate a slight increase in both a and c unit-cell parameters with synthesis temperature, whereas the $c/3a$ ratio remains almost constant. The $c/3a$ ratio actually measures

(8) Thackeray, M. M.; Kang, S.-H.; Johnson, C. S.; Vaughey, J. T.; Benedek, R.; Hackney, S. A. *J. Mater. Chem.* **2007**, *17*, 3112.
(9) Chernova, N. A.; Ma, M.; Xiao, J.; Whittingham, M. S.; Breger, J.; Grey, C. P. *Chem. Mater.* **2007**, *19*, 4682.
(10) Larsom, A. C.; Dreele, R. B. V. General Structure Analysis System (GSAS); Los Alamos National Laboratory Report LAUR 86-748; Los Alamos National Laboratory: Los Alamos, NM, 2004.

Table 1. Ratio of Li to Transition Metals Found from DCP Analysis, Rietveld Refinement Results, BET Surface Areas, And Average Effective Magnetic Moment of Transition Metal Ions for $LiNi_{0.45}Mn_{0.45}Co_{0.1}O_2$ Prepared at Different Temperatures

temp (°C)	Li/M ratio	*a* (Å)	*c* (Å)	*c*/3*a*	Ni % on Li sites	R_p (%)	BET (m^2/g)	μ_{exp}, μ_B
700	0.97	2.872(1)	14.246(3)	1.653	7.7	6.0	11.1	3.03
800	0.98	2.872(2)	14.256(2)	1.655	6.2	5.9	5.1	3.13
900	1.00	2.874(2)	14.270(1)	1.655	6.3	6.2	2.0	3.20
1000	0.93	2.878(2)	14.280(5)	1.654	5.8	6.3	0.7	3.21

the layered-ness of the structure reflecting the deviation of the lattice from a perfect cubic close-packed one. An ideal ccp lattice has a *c*/3*a* ratio of 1.633 while an ideal layered lattice with no transition metal in the lithium layer has a *c*/3*a* ratio of 1.672 for TiS_2. When lithium is intercalated, this ratio increases to 1.793 for $LiTiS_2$.[11] The closer the *c*/3*a* value is to 1.633, the more transition metal is present in the lithium layer. The *c*/3*a* ratio in Table 1 does not vary significantly for these four samples studied, which means the synthesis temperature has surprisingly little influence on the extent of Ni/Li disorder. The Rietveld refinement (Table 1) reveals about 6% of Ni in the Li layer (Ni_{Li}) throughout the series, which is consistent with the conclusion from the *c*/3*a* ratio analysis. Jiang et al. reported similar result for cobalt-rich compound.[12]

To rationalize the observed trend in cell parameters, we have studied the effect of the synthesis temperature on the sample composition using DCP analysis and magnetic properties; the latter is used to determine the oxidation states of the transition metals. DCP results indicate that both 700 and 1000 °C samples are noticeably Li-deficient (Table 1), the samples synthesized at 800 and 900 °C are nearly stoichiometric. The Ni:Mn:Co ratio is close to the intended 9:9:2 for all the samples. The materials are paramagnetic above 250 K, and so the effective magnetic moment μ_{eff} can be determined using the Curie−Weiss law $\chi = N_A\mu_{eff}^2/3k_B(T-\Theta)$, where N_A is Avogadro's number, k_B the Boltzmann constant, and Θ the Curie−Weiss temperature (Figure 2). The μ_{eff} values obtained from these fits increase with increasing synthesis temperature (Table 1). The stoichiometric 900 °C sample has $\mu_{eff} = 3.20\ \mu_B$, which is very close to the 3.22 μ_B expected for Ni^{2+} ($S = 1$, $\mu = 3.87\ \mu_B$) and Mn^{4+} ($S = 3/2$, $\mu = 3.87\ \mu_B$) oxidation states. It is interesting to note that μ_{eff} of the Li-deficient 700 °C sample is smaller than the theoretical value, whereas the 1000 °C material, which is also Li-deficient, has a higher effective magnetic moment. These values can be rationalized if different mechanisms of Li-deficiency are involved. At low temperatures, a Li_xMO_2 ($x < 1$, M=$Ni_{0.45}Mn_{0.45}Co_{0.1}$) compound is formed where part of the Ni^{2+} ($S = 1$) oxidized to Ni^{3+} ($S = 1/2$) with lower μ_{eff}. The poor splitting between the 018 and 110 peaks found in the XRD pattern suggests some spinel-like character to the structure. In the 1000 °C sample, the Li-deficiency should be accompanied by more transition metals residing on the Li sites as in $[Li_xM_{1-x}]MO_2$ ($x < 1$). In this case part of the Co^{3+} ($S = 0$) is reduced to Co^{2+} (S=1/2) leading to the increase of the magnetic moment. The decreased μ_{eff} value of the 800 °C sample is consistent with slight lithium deficiency when part of the Ni^{2+} is oxidized to Ni^{3+}. These assignments are confirmed by the trend observed in the *a* and *c* lattice parameters: oxidation of Ni^{2+} to Ni^{3+} at the lower synthesis temperature leads to a smaller cell, while reduction of Co^{3+} to Co^{2+} at high temperatures leads to larger cell. The magnetic properties of $LiNi_{0.45}Mn_{0.45}Co_{0.1}O_2$ will be discussed in detail later in the paper together with intentionally nonstoichiometric $Li_{1+z}M_{1-z}O_2$ samples to provide more bases for comparison.

The BET surface area (Table 1) of the samples shows a rapid decrease from 11.1 m^2/g to only 0.7 m^2/g as the synthesis temperature increases. The sample synthesized at 800 °C gives a specific surface area of 5.1 m^2/g. In other words, high temperature facilitates formation of material with improved layered structure, but lower surface area. The TEM images in Figure 3 confirm that the particle size increases with synthesis temperature. At 700 °C the particles do not show a specific morphology and the average particle diameter is less than 100 nm. As the temperature increases to 800 °C the hexagonal shape becomes clear and the particle size increases rapidly to 750 nm at 1000 °C. The well-defined edges of the particles prepared at 1000 °C are in agreement with their high crystallinity. Particle size discussed here is the size of discrete particle, whereas the crystallite size is

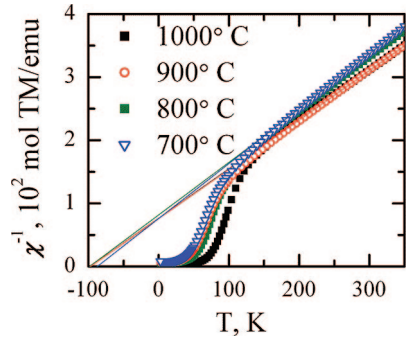

Figure 2. Temperature dependences of the reciprocal susceptibility of $LiNi_{0.45}Mn_{0.45}Co_{0.1}O_2$ synthesized at various temperatures and their fit to the Curie−Weiss law (solid lines).

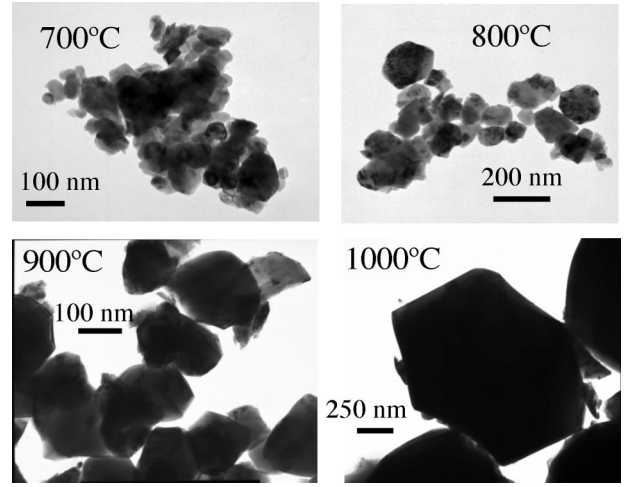

Figure 3. TEM images of $LiNi_{0.45}Mn_{0.45}Co_{0.1}O_2$ synthesized from 700−1000 °C.

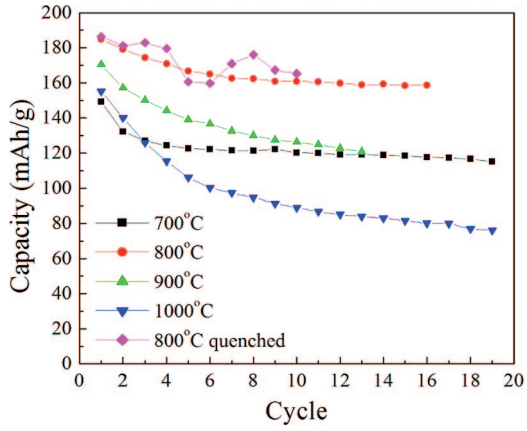

Figure 4. Comparison of the electrochemical capacity of $LiNi_{0.45}Mn_{0.45}Co_{0.1}O_2$ prepared at different temperatures. A sample quenched from 800 °C is shown for comparison. All the cells were cycled between 2.5 and 4.6 V at 0.5 mA/cm^2.

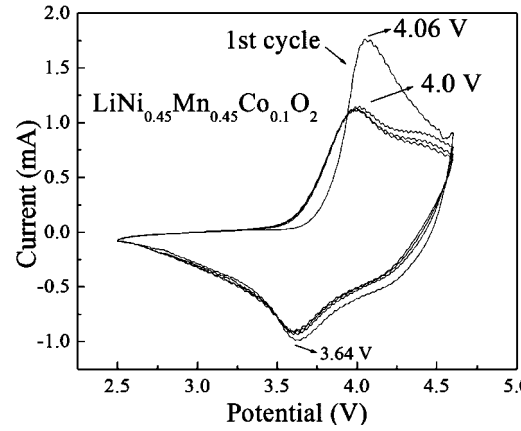

Figure 5. Cyclic voltammetry of Li/$LiNi_{0.45}Mn_{0.45}Co_{0.1}O_2$ formed at 800 °C at a sweeping rate of 0.1 mV/s between 2.5 and 4.6 V.

the size of the effective crystal domain, which contributes coherently to the diffraction experiment. One can calculate the grain size at different orientations for these four compounds from their line-width in Figure 1 by using Scherrer's formula: $D=0.89\lambda/\beta\cos\theta$, where λ is the wavelength of the X-rays (0.1541 nm), β in radian is the peak width at half-maximum height, θ is the Bragg's angle. The grain size estimated at 003 peak increases from 20 to 80 nm as the synthesis temperature increases, which is consistent with our observation from the XRD pattern and TEM images.

Usually, small particles with high surface areas facilitate the diffusion of the lithium ions during charging and discharging and thus satisfy the requirements for high rate applications.[13] But if the particle size is decreased to the nanolevel, a high reactivity due to the large surface area may lead to safety problems and decrease the thermal stability of the material.[14] The electrochemical behavior of $LiNi_{0.45}Mn_{0.45}Co_{0.1}O_2$ synthesized at different temperatures is compared in Figure 4. The sample prepared at 800 °C shows both the highest initial capacity of 180 mAh/g when cycled between 2.5 and 4.6 V at 0.5 mA/cm^2 and the most stable cycling among the four. The initial efficiency of the cell using the 800 °C sample is about 87%. After the first cycle, the efficiencies between charge and discharge were close to 100%. However, the capacity faded gradually and about 86% of the initial discharge capacity was retained at the 16th cycle. The sample prepared at 900 °C delivers about 170 mAh/g capacity in the first cycle, which is less than that of the 800 °C sample. The poor capacity maintenance of $Li[Ni_{0.45}Mn_{0.45}Co_{0.1}]O_2$ prepared at 1000 °C is probably due to the large particles formed at high temperature, which prolongs the lithium diffusion path while cycling. Thus, 800 °C was chosen as the optimum synthesis temperature to prepare all the compounds reported here.

To ascertain whether the rate of cooling from the synthesis temperature of 800 °C had any impact on the structure and electrochemical behavior, one sample was quenched between copper plates whereas another was allowed to cool in the furnace after it was switched off. The lattice parameters (a = 2.871 Å and c = 14.254 Å) of the quenched sample are almost equal to those of the slow-cooled one considering the typical errors. Rietveld refinement reveals that the cation disorder of the quenched sample is about 6.8% very close to that of the slow-cooled one at 6.2%; the magnetic properties of the samples are also very similar. The cycling ability for the quenched $LiNi_{0.45}Mn_{0.45}Co_{0.1}O_2$ is presented in Figure 4 for comparison. Both the 800 °C slow-cooled and the quenched sample show an initial discharge capacity higher than 180 mAh/g, the first few cycles are very close and there is no obvious difference in the cycling stability, and after 10 cycles they both have a capacity of 160 mAh/g. Thus, we conclude that slow or fast cooling has no effect on the electrochemical behavior, consistent with our refinement results and an earlier report for other compositions of these layered compounds.[15]

To further understand the electrochemical reactions occurred in the charge−discharge process, the cyclic voltammogram at a sweep rate of 0.1 mV/s is shown in Figure 5. The first oxidation peak is observed at 4.06 V and then it shifts to 4.0 V in the following cycles and the major reduction peaks are always around 3.64 V. They correspond to the oxidation and reduction between Ni^{2+} and Ni^{4+}. The difference between the major redox peak potentials is less than 0.4 V, which is consistent with the polarization between charge and discharge curves. Different behavior observed in the first cycle may be caused by some irreversible reactions like the formation of the SEI film. An additional pair of redox peaks could be seen after the first oxidation cycle. This pair of peaks is related to the transition between Co^{3+} and Co^{4+}, which happens at a voltage higher than 4.0 V. The absence of the redox peak at around 3 V confirms that manganese in our compound is in the 4+ state instead of 3+ state, which is electrochemically inactive.

The theoretical capacity of $Li[Ni_{0.45}Mn_{0.45}Co_{0.1}]O_2$ is 279.3 mAh/g if all the lithium can be cycled, and 251.4 mAh/g if only the nickel is redox active. To determine the experimental

(11) Whittingham, M. S.; Gamble, F. R. *Mater. Res. Bull.* **1975**, *10*, 363.
(12) Jiang, J.; Buhrmester, T. W.; Eberman, K. J.; Krause, L.; Dahn, J. R. *J. Electrochem. Soc.* **2005**, *152*, A19.
(13) Horiba, T.; Hironaka, K.; Matsumura, T.; Kai, T.; Koseki, M.; Muranaka, Y. *J. Power Sources* **2003**, *119*, 893.
(14) Cho, J.; Park, B. *J. Power Sources* **2001**, *92*, 35.
(15) Lu, Z.; Beaulieu, L. Y.; Donaberger, R. A.; Thomas, C. L.; Dahn, J. R. *J. Electrochem. Soc.* **2002**, *149*, A778.

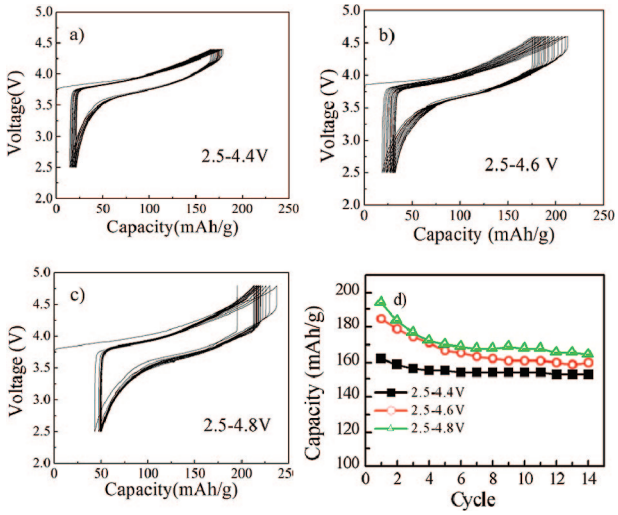

Figure 6. $LiNi_{0.45}Mn_{0.45}Co_{0.1}O_2$ cycled between (a) 2.5 and 4.4 V, (b) 2.5 and 4.6 V, and (c) 2.5 and 4.8 V at 0.5 mA/cm^2. (d) Comparison of cycling capacities for these three voltage ranges.

capacity, we cycled cells at 0.5 mA/cm^2 between 2.5 and a charge limit of 4.4, 4.6, and 4.8 V. The higher charging voltages would allow more lithium to be removed, but at the expense of possible side reactions with the electrolyte. The results are shown in Figure 6. When cycled between 2.5 and 4.4 V, the cathode material gives an initial discharge capacity of around 160 mAh/g, the irreversible capacity in the first cycle is about 20 mAh/g. When the material is cycled between 2.5 and 4.6 V, its capacity increases to around 180 mAh/g but its irreversible capacity also increases to 30 mAh/g. The sample cycled between 2.5 and 4.8 V delivers the largest capacity of about 200 mAh/g; however, the irreversible capacity increases to 50 mAh/g while the polarization becomes the largest. The increase in capacity with increasing cutoff voltage can be explained by more lithium ions being deintercalated upon charge, thus allowing more lithium ions to be intercalated in the layered structure upon discharge. This leads to an increase in both the charge and discharge capacities, but to a larger first cycle loss, that might be associated with surface reactions and decomposition of the electrolyte. Although the higher cutoff voltage gives a higher capacity, it decays faster. Cycling between 2.5 and 4.4 V (Figure 6d) shows the most stable behavior among the three. The capacity retention is as high as 94.3% after 14 cycles, whereas the capacity retention for the 4.6 and 4.8 V cutoff voltages are 85.8 and 84.3%, respectively. Both the instability of the electrolyte and the structure of this material itself contribute to the fast fading rate at high potential.

The effect of the charge cutoff voltage on the electrochemical behavior of the related compound $LiNi_{0.4}Mn_{0.4}Co_{0.2}O_2$ with higher Co content was previously published by our group.[6] The coin cells were investigated at a current density of 0.25 mA/cm^2 (*C*/10 rate) for voltage limits of 4.4, 4.5, 4.6, 4.7, and 4.8 V. The corresponding capacities in the first cycle are 163.3, 175.6, 184.2, 199.3, and 202.6 mAh/g, respectively. The results are similar to those observed for $LiNi_{0.45}Mn_{0.45}Co_{0.1}O_2$. This voltage-dependent property may be used to give some overcharge protection in the

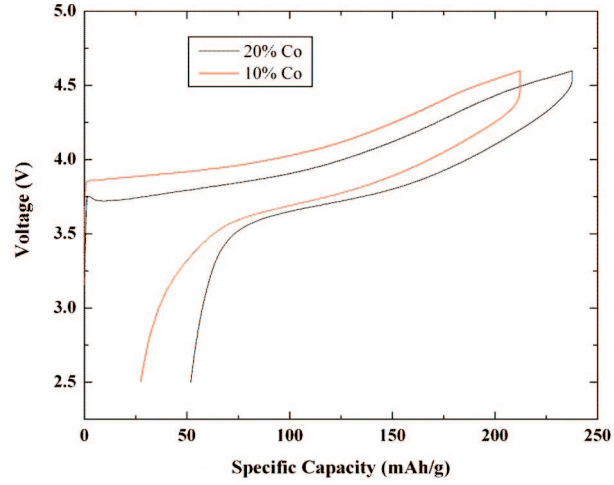

Figure 7. Comparison of the first cycle for $LiNi_{0.45}Mn_{0.45}Co_{0.1}O_2$ and $LiNi_{0.4}Mn_{0.4}Co_{0.2}O_2$ cycled at 0.5 mA/cm^2.

practical cells. Figure 7 compares the details of the first cycle for $LiNi_{0.45}Mn_{0.45}Co_{0.1}O_2$ and $LiNi_{0.4}Mn_{0.4}Co_{0.2}O_2$. The first charge capacity of $LiNi_{0.4}Mn_{0.4}Co_{0.2}O_2$ (ca. 230 mAh/g) is a little bit higher than that of $LiNi_{0.45}Mn_{0.45}Co_{0.1}O_2$ (ca. 210 mAh/g), but its first irreversible capacity is also larger at around 50 mAh/g leading to little difference in the first discharge (ca. 180 mAh/g) between compounds containing 10 and 20% cobalt. However, a smaller polarization is observed for $LiNi_{0.4}Mn_{0.4}Co_{0.2}O_2$ than for $LiNi_{0.45}Mn_{0.45}Co_{0.1}O_2$. The slightly higher charge and discharge plateau in $LiNi_{0.45}Mn_{0.45}Co_{0.1}O_2$ should be related to the increasing Mn content, which will be the subject of a separate publication. Both $LiNi_{0.45}Mn_{0.45}Co_{0.1}O_2$ and $LiNi_{0.4}Mn_{0.4}Co_{0.2}O_2$ could deliver as high of capacities as those reported for $LiNi_{1/3}Mn_{1/3}Co_{1/3}O_2$, with even more stable cycling.[16] Delmas reported the electrochemistry of $LiNi_{0.425}Mn_{0.425}Co_{0.15}O_2$ synthesized by several different methods.[17] This compound delivers similar charge−discharge capacities in the first few cycles but decays faster than that of our $LiNi_{0.45}Mn_{0.45}Co_{0.1}O_2$ compound when the same hydroxide method is used. Delmas' compounds were synthesized at 1000 °C, which resulted in larger particles than that of our sample prepared at 800 °C. Partial substitution of cobalt by aluminum as in $LiNi_{0.4}Mn_{0.4}Co_{0.15}Al_{0.05}$ delivers an initial discharge capacity about 160 mAh/g at a 3*C* rate (~5 mA/cm^2) between 2.0 and 4.3 V,[7] with only a small sacrifice of capacity.

The lower amount of Co in $LiNi_{0.45}Mn_{0.45}Co_{0.1}O_2$ leads to an increased nickel content in the lithium layer, but not as high as in $LiNi_{0.5}Mn_{0.5}O_2$. As a result, the MO_2 layers are pinned together, and no formation of the one block 1T structure was observed as opposed to $LiNi_{0.33}Mn_{0.33}Co_{0.33}O_2$. Further reduction of the Co content would likely lead to some reduction of electrochemical capacity and cycleability, especially at high current density, as found in $LiNi_{0.5}Mn_{0.5}O_2$.[4]

Variation in Initial Lithium Content. To understand the effect of lithium content on the transition metal distribution

(16) Patoux, S.; Doeff, M. *Electrochem. Commun.* **2004**, *6*, 767.
(17) Tran, N.; Croguennec, L.; Jordy, C.; Biensan, P.; Delmas, C. *Solid State Ionics* **2005**, *176*, 1539.

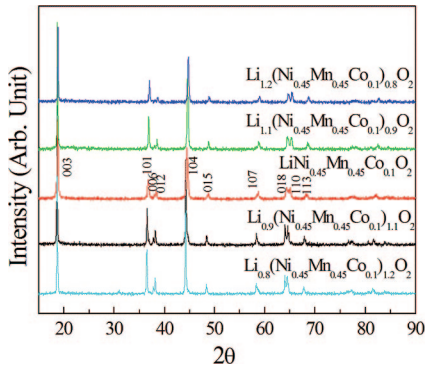

Figure 8. XRD patterns for $Li_{1+z}[Ni_{0.45}Mn_{0.45}Co_{0.1}]_{1-z}O_2$, $0.8 \le 1 + z \le 1.2$.

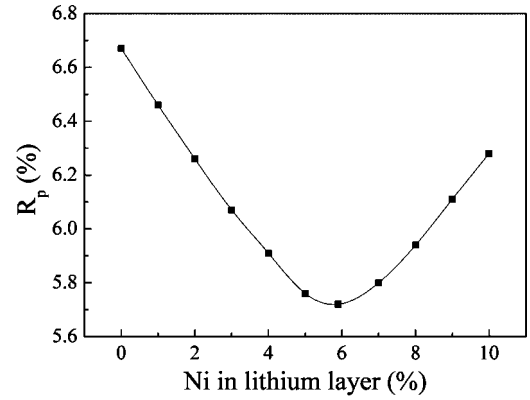

Figure 9. Profile *R*-factor of the Rietveld refinement of $LiNi_{0.45}Mn_{0.45}Co_{0.1}O_2$ scanned with step size of 0.02° and exposure of 10 s vs cation disorder extent between nickel and lithium ions. The line is guide to the eye.

and electrochemical properties of this material, we made a series of materials with the composition $Li_{1+z}[Ni_{0.45}Mn_{0.45}Co_{0.1}]_{1-z}O_2$, $0.8 \le 1 + z \le 1.2$. All the compounds appear single phase with layered structure (Figure 8) except for the compound $Li_{0.8}[Ni_{0.45}Mn_{0.45}Co_{0.1}]_{1.2}O_2$ with the lowest lithium content, for which an additional phase, probably with the spinel structure, was observed. All the X-ray diffraction peaks shift to higher angle and the splitting of the 018 and 110 peaks becomes more significant with increasing lithium content, which indicates the formation of a more ordered layered structure with smaller *d*-spacing because of more effective suppression of the electrostatic repulsion between the transition metal layers with increasing Li content. The Rietveld refinement of the X-ray diffraction data was performed for this series assuming α-$NaFeO_2$ structure; the cell parameters are shown in Table 2 together with the DCP analysis results. The DCP analysis results show that the actual stoichiometry of each sample is very close to the target value, which means that 5% excess amount of lithium in the starting material is necessary to get the desired lithium content in the final product. Starting from $Li_{0.9}[Ni_{0.45}Mn_{0.45}Co_{0.1}]_{1.1}O_2$, both *a* and *c* parameters begin to decrease, whereas the *c*/3*a* ratio increases with increasing lithium content. For a pure spinel phase such as $LiMn_2O_4$, the cubic close-packed lattice is closely related to the α-$NaFeO_2$ layer structure, differing only in the distribution of the cations among available octahedral and tetrahedral sites.[4] In the layers containing both Li and Mn ions, 1/3 of the octahedral sites are occupied by Mn, whereas Li ions reside in the tetrahedral sites. Thus, because of the partial formation of a spinel structure, an apparent cation disorder value of about 19% as observed in $Li_{0.8}[Ni_{0.45}Mn_{0.45}Co_{0.1}]_{1.2}O_2$ actually reflects the percentage of both Ni and Mn ions in the Li layers and is reasonably the largest in Table 2. The increase of the *c*/3*a* ratio suggests that less Ni^{2+} are occupying the normal Li^+ sites in the compounds with excess lithium. This is consistent with the structure refinement results, which show a rapid decrease in nickel content in the lithium layer with increasing lithium content.

We have checked the sensitivity of the Rietveld analysis for determination of the Li/Ni exchange keeping in mind that 1% of the nickel corresponds to only 0.5% of all electrons in the system. In Figure 9, we compare the sensitivity of R_p to the variation of Ni content in the lithium layer for the X-ray diffraction pattern scanned over the range of 10−90° 2θ with a step size of 0.02° and exposure of 10 s. The Rietveld refinement gives 5.9% of Ni in the Li layer with $R_p = 5.7\%$. After the refinement, we fixed the Ni% in the lithium sites manually from 0 to 10% and did the refinement again to see how the final R_p value changes. One can observe that the curve has a pronounced minimum, which means R_p is quite sensitive to the extent of the cation disorder between the nickel and lithium ions when using a long exposure time with less background noise. There is about 2% error in these refinements, and we believe the overall trend for the series of samples is reliable.

We have further confirmed the results of the Rietveld refinement using the magnetic properties. The temperature dependences of the magnetic susceptibility of the $Li_{1+z}[Ni_{0.45}Mn_{0.45}Co_{0.1}]_{1-z}O_2$ materials (for $1 + z > 1.0$) obey the Curie−Weiss law above 100 K, as shown in Figure 10. For the lower lithium contents, the Curie−Weiss behavior is observed only above 250 K, which is indicative of stronger magnetic interactions. The effective magnetic moments μ_{eff} and the absolute values of the Curie−Weiss temperature Θ both decrease with increasing Li content (Table 3). The average oxidation state of the transition metals increases with the lithium content in order to maintain the charge balance. Thus, when the lithium content is larger than 1.0, the increase of the oxidation state is caused by the oxidation of Ni^{2+} ($S = 1$, $\mu = 2.83\ \mu_B$) to Ni^{3+} ($S = 1/2$, $\mu = 1.73\ \mu_B$) and then

Table 2. DCP and Rietveld Refinement Results

compd	Li from DCP	*a* (Å)	*c* (Å)	*c*/3*a*	R_p (%)	Ni % on lithium sites
$Li_{0.8}[Ni_{0.45}Mn_{0.45}Co_{0.1}]_{1.2}O_2$	0.83	2.885(2)	14.259(5)	1.647	7.4	19.4
$Li_{0.9}[Ni_{0.45}Mn_{0.45}Co_{0.1}]_{1.1}O_2$	0.90	2.885(0)	14.303(1)	1.653	6.0	9.0
$Li[Ni_{0.45}Mn_{0.45}Co_{0.1}]O_2$	0.98	2.872(2)	14.256(2)	1.655	5.9	6.2
$Li_{1.1}[Ni_{0.45}Mn_{0.45}Co_{0.1}]_{0.9}O_2$	1.06	2.859(8)	14.222(1)	1.658	5.3	1.9
$Li_{1.2}[Ni_{0.45}Mn_{0.45}Co_{0.1}]_{0.8}O_2$	1.17	2.854(7)	14.207(5)	1.659	5.3	0.7

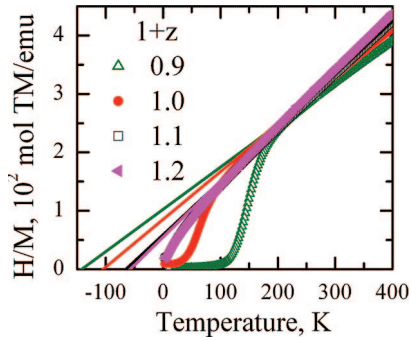

Figure 10. Temperature dependences of the reciprocal susceptibility and their fit to the Curie−Weiss law (straight lines). The label indicates lithium content $1 + z$ in $Li_{1+z}(Ni_{0.45}Mn_{0.45}Co_{0.1})_{1-z}O_2$.

to Ni^{4+}($S = 0$, $\mu = 0$) accompanied by a decrease of the magnetic moment. On the other hand, the observed increase of magnetic moment when the lithium content becomes less than 1.0 is the result of the reduction of Co^{3+} ($S = 0$, $\mu = 0$) to Co^{2+} ($S = 1/2$, $\mu = 1.73\ \mu_B$) and Mn^{4+} ($S = 3/2$, $\mu = 3.87\ \mu_B$) to Mn^{3+} ($S = 2$, $\mu = 4.90\ \mu_B$) resulting in the increase of average magnetic moment. The magnetic moments calculated using these assumptions are in satisfactory agreement with the experimentally observed values (Table 3). This further validates the previous use of magnetic properties in determination of structure and composition of $LiNi_{0.45}Mn_{0.45}Co_{0.1}O_2$ synthesized at various temperatures.

To address the evolution of the Li/Ni disorder in the $Li_{1+z}[Ni_{0.45}Mn_{0.45}Co_{0.1}]_{1-z}O_2$ series we have studied the magnetization curves of the samples. The Ni ions in the TM layers facilitate the formation of ferrimagnetic clusters, which leads to an increase of the magnetic hysteresis observed at low temperatures. In accordance with this assumption, the lithium-excess compounds with negligible amount of Ni/Li exchange show linear magnetization without any hysteresis (Figure 11). A small hysteresis loop is observed in the stoichiometric compound. For $Li = 0.9$, a large hysterysis loop appears with remanent magnetization $M_r \approx 1000$ emu/mol and a coercive field $H_c \approx 0.3$ T. Interestingly, when the Li content is further decreased to 0.8, the hysterysis loop becomes narrower with a smaller coercive field of $H_c \approx 0.08$ T, whereas the M_r remains close to that of $Li_{0.9}[Ni_{0.45}Mn_{0.45}Co_{0.1}]_{1.1}O_2$. As narrow hysteresis loops are often found in ferrimagnetic spinels, we synthesized a compound with $1 + z = 0.5$, which is a spinel with lattice parameter $a = 8.187(1)$ Å. The shape of the hysteresis loop in this compound changes dramatically: it becomes very narrow, with almost zero coercivity, and the magnetization saturates at high field at $M_s \approx 2790$ emu/mol TM, which is equivalent to magnetic moment of 0.5 μ_B per TM ion. A similar hysteresis loop was observed in the $LiMn_{1.5}Ni_{0.5}O_4$ spinel.[18] Thus, both XRD and magnetic data indicate an increase of the amount of Ni in the Li layer with decreasing Li content and coexistence of a spinel phase for $1 + z \leq 0.8$ in $Li_{1+z}[Ni_{0.45}Mn_{0.45}Co_{0.1}]_{1-z}O_2$.

Figure 12 compares the electrochemical properties of this series of samples. It is noticeable that $Li_{0.9}[Ni_{0.45}Mn_{0.45}Co_{0.1}]_{1.1}O_2$ shows very good electrochemical behavior. Here, 10% of the lithium sites will be occupied by nickel, in agreement with the Rietveld value of 9 ± 2%. The initial discharge capacity is more than 180 mAh/g and its first 10 cycles are the most stable among all the samples. The first cycle irreversible capacity is about 25 mAh/g and the polarization is around 0.4 V. On the other hand, when the lithium content is as low as 0.8 or as high as 1.1, the capacity of the material decreases rapidly and poor electrochemical behavior is observed. A long plateau appears at about 4.0 and 3.7 V during charging and discharging, respectively, corresponding to the deintercalation and intercalation of the lithium ions. Interestingly, the first charging capacity increases with the increase of lithium content while the first discharge capacity does not show the same trend. The differential capacity vs voltage for $Li/Li_{1+z}[Ni_{0.45}Mn_{0.45}Co_{0.1}]_{1-z}O_2$ cells cycled between 2.5 and 4.6 V using a current density of 0.5 mA/cm^2 in Figure 13 gives us more details about their electrochemical behavior. The peaks in Figure 13 correspond to the plateaus in Figure 12. The materials with lithium contents of 0.9 (Figure 13b) and (Figure 13c) have similar patterns with a major peak around 4.0 V and additional peaks at 4.4 V corresponding to the transition between Ni^{2+}/Ni^{4+} and Co^{3+}/Co^{4+} couples, respectively. The difference ΔV between the major peaks is related to the polarization in Figure 12. One can observe that ΔV for $1 + z = 0.8$ (Figure 13a) is as large as 0.7 V, which can be associated with the existence of multiple phases. ΔV decreases rapidly to only around 0.4 V when $1 + z = 0.9$ or 1.0 but develops further as $1 + z = 1.1$ (Figure 13d). When the lithium content is equal to 1.1 (Figure 13d) or 1.2 (Figure 13e), the two redox peaks change into a broad one and a sharp peak at 4.5 V appeared during the first charge. Notice that this peak only appears in the first charge profile, after which the differential capacity vs voltage becomes stable. It is also this extra peak that contributes to the increase of the first charge capacity in Figure 12. The capacity associated with this peak is irreversible and may be related the simultaneous extraction of Li and O during the first charge.

Because the actual lithium to transition metal ratio in $Li_{1+z}[Ni_{0.45}Mn_{0.45}Co_{0.1}]_{1-z}O_2$, ($1 + z = 1.1$) is much higher than 1.0 ($(1 + z)/(1 - z) = 1.22$), $Li_{1.024}(Ni_{0.45}Mn_{0.45}Co_{0.1})_{0.976}O_2$ where Li/TM = 1.05 was prepared and compared with the other lithium rich compound. Figure 14 (left) shows the charge−discharge curves of the $Li_{1.024}(Ni_{0.45}Mn_{0.45}Co_{0.1})_{0.976}O_2$ cathode. In the first cycle, it gives a discharge capacity of more than 180 mAh/g, whereas the polarization is less than 0.4 V. When the cycling current is reduced from 0.5 to 0.1 mA/cm^2 in Figure 14 (right), both the initial charge and discharge capacities are increased to 250 and 194 mAh/g, respectively. The polarization is further reduced to only 0.3 V. The extended cycling behavior of this lithium-rich compound is compared with the lithium stoichiometric material, and with $LiNi_{0.4}Mn_{0.4}Co_{0.2}O_2$[6] in Figure 15. The $Li_{1.024}(Ni_{0.45}Mn_{0.45}Co_{0.1})_{0.976}O_2$ and stoichiometric $LiNi_{0.45}Mn_{0.45}Co_{0.1}O_2$ electrodes show an initial capacity of around 180 mAh/g between 2.5 and 4.6 V when using a current density of 0.5 mA/cm^2. $Li_{1.024}(Ni_{0.45}Mn_{0.45}Co_{0.1})_{0.976}O_2$ gives an enhanced capacity over the first 10 cycles

(18) Nakamura, T.; Yamada, Y.; Tabuchi, M. *J. Appl. Phys.* **2005**, *98*, 093905.

Table 3. Magnetic Parameters of $Li_{1+z}(Ni_{0.45}Mn_{0.45}Co_{0.1})_{1-z}O_2$ Samples

$1+z$	C (emu K/mol TM)	Θ (K)	μ_{exp}, μ_B	μ_{theor}, μ_B	M_r (emu/mol TM)	H_c (Oe)	T_b (K)
1.2	1.042(1)	−57.4(2)	2.89	2.82	0.7(1)	16.5(1)	7.0(5)
1.1	1.095(1)	−64.8(2)	2.96	3.04	1.1(1)	24.1(1)	7.5(5)
1.0	1.225(1)	−104.5(3)	3.13	3.22	35.8(1)	459(1)	65(2)
0.9	1.383(2)	−142.1(3)	3.33	3.37	777.7(1)	2700(5)	165(2)

and then gradually becomes the same as the stoichiometric one between 10 and 25 cycles. At the 50th cycle, their capacities drop to around 120 and 130 mAh/g for $Li_{1.024}(Ni_{0.45}Mn_{0.45}Co_{0.1})_{0.976}O_2$ and $LiNi_{0.45}Mn_{0.45}Co_{0.1}O_2$, respectively. Thus $LiNi_{0.45}Mn_{0.45}Co_{0.1}O_2$ holds its capacity better than $Li_{1.024}$ $(Ni_{0.45}Mn_{0.45}Co_{0.1})_{0.976}O_2$ but with a slightly lower capacity in the first few cycles. The $LiMn_{0.4}Ni_{0.4}Co_{0.2}O_2$ electrode, which was cycled between 2.5 and 4.4 V at 0.12 mA/cm^2, showed a higher capacity retention,[6] but that is probably partly related to the lower cutoff charge voltage and current density used (4.4 V and 0.12 mA/cm^2). Thus, these three compositions show comparable behavior.

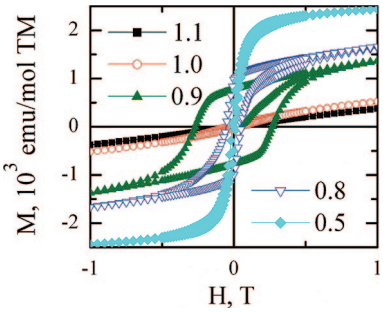

Figure 11. Magnetization curves of $Li_{1+z}(Ni_{0.45}Mn_{0.45}Co_{0.1})_{1-z}O_2$. The label indicates Li content $1+z$.

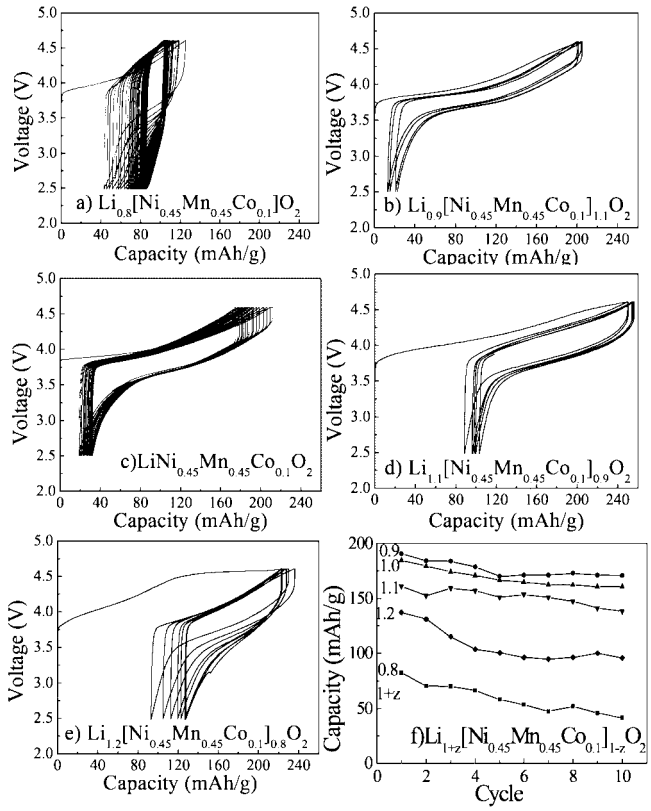

Figure 12. Electrochemical behavior of $Li_{1+z}[Ni_{0.45}Mn_{0.45}Co_{0.1}]_{1-z}O_2$, $0.8 \le 1+z \le 1.2$ at 0.5 mA/cm^2 cycled between 2.5 and 4.6 V.

To establish the relation between the structure and electrochemical performance in the $Li_{1+z}(Ni_yMn_yCo_{1-2y})_{1-z}O_2$ series, the initial lithium and transition metal ion distribution along with ion migration during cycling should be carefully considered. As previously established, with decreasing lithium and Co content, more Ni^{2+} ions migrate to the lithium layer. In Li-stoichiometric compounds ($1+z=1$) an equal amount of Li is found in the TM layer (Li_{TM}) as Ni in the Li layer, while in the Li-deficient compounds ($1+z<1$) more Ni ions are found in the Li layer than Li ions in the TM layer. For example, the $1+z=0.9$ compound with 8−9% of Ni in the Li layer may have very little Li in the TM layer, approaching the composition $[Li_{0.9}Ni_{0.1}]Ni_{0.95}Mn_{0.495}Co_{0.11}]O_2$.

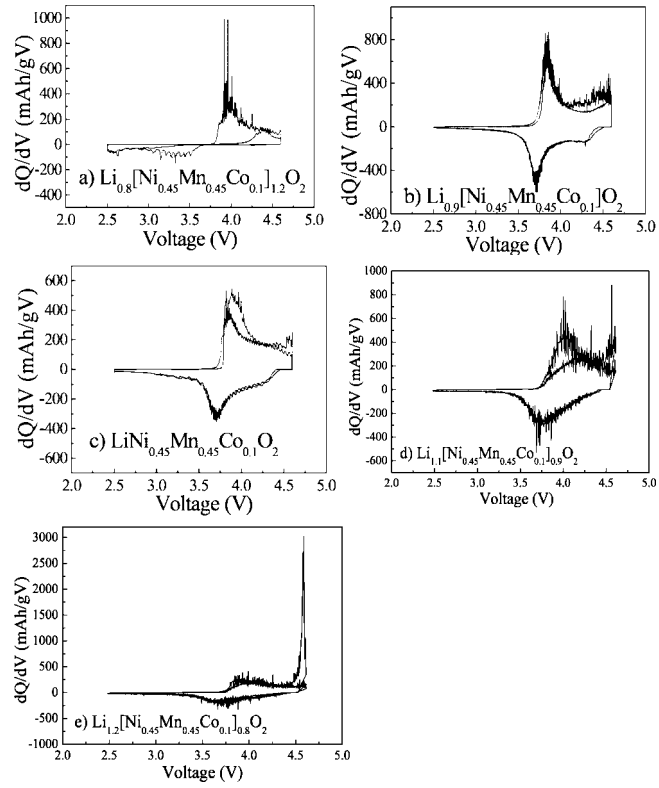

Figure 13. Differential capacity vs voltage of Li/$Li_{1+z}[Ni_{0.45}Mn_{0.45}Co_{0.1}]_{1-z}O_2$ ($0.8 \le 1+z \le 1.2$) cells cycled between 2.5 and 4.6 V.

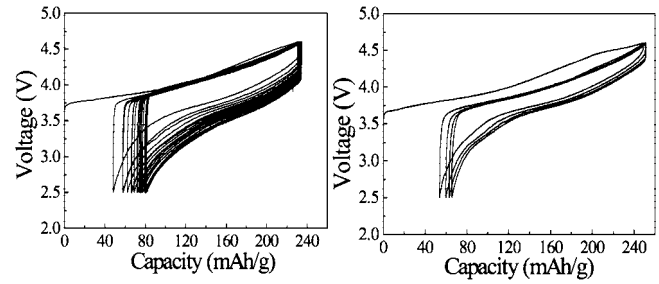

Figure 14. Charge−discharge curves for $Li_{1.024}(Ni_{0.45}Mn_{0.45}Co_{0.1})_{0.976}O_2$ cycled between 2.5 and 4.6 V at 0.5 mA/cm^2 (left) and 0.1 mA/cm^2 (right).

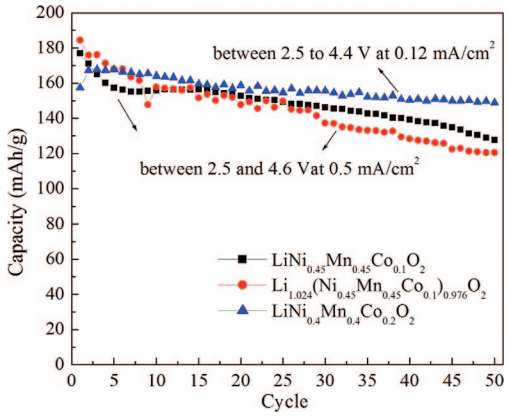

Figure 15. Comparison of cycling ability for $Li_{1.024}(Ni_{0.45}Mn_{0.45}Co_{0.1})_{0.976}O_2$, $LiNi_{0.45}Mn_{0.45}Co_{0.1}O_2$, and $Li/LiMn_{0.4}Ni_{0.4}Co_{0.2}O_2$. Note that different rates and voltage range were used as indicated in the figure.

It has been commonly believed that in the layered oxides the Ni/Li site exchange must be as low as possible for the easy transportation of lithium.[19] On the basis of the excellent electrochemical properties of $LiNi_{0.4}Mn_{0.4}Co_{0.2}O_2$ with 4% Ni/Li exchange[20] and of $LiNi_{0.5}Mn_{0.5}O_2$ with 8−9% of cation disorder,[21] we have suggested that the existence of a small amount of Ni^{2+} in the normal lithium layers helps to pin the layered structure together, which makes the structure more stable while cycling. It has been established from the neutron diffraction studies that both Ni in the Li layer (Ni_{Li}) and Li in the transition metal layer (Li_{TM}) are active and migrate upon cycling of this material. Li_{TM} moves to the tetrahedral sites of the Li layer early in the charge process, forming so-called Li-dumbbells. These tetrahedral Li ions can only be removed above 4.6 V, and as that happens Ni_{Li} ions migrate back to the TM layer.[22,23] This is in agreement with our findings of better electrochemical performance of Li-deficient $Li_{0.9}[Ni_{0.45}Mn_{0.45}Co_{0.1}]_{1.1}O_2$ in comparison with stoichiometric or Li-excess compounds. In this case we get rid of the problematic Li_{TM}, which forms tetrahedral dumbbells reducing Li diffusion. At the same time Ni_{Li} cannot migrate back to the TM layer, as there are no vacancies, and the overall structural stability upon cycling is enhanced this way. Thus, 8−9% is an appropriate amount of Ni in the Li layer to pin the structure together while providing excellent electrochemistry. The excess amount of Li ions in either $Li_{1.1}[Ni_{0.45}Mn_{0.45}Co_{0.1}]_{0.9}O_2$ or $Li_{1.2}[Ni_{0.45}Mn_{0.45}Co_{0.1}]_{0.8}O_2$ does not give additional capacity but, just the opposite, it reduces the attainable capacities for both at current densities of 0.5 mA/cm^2 at room temperature. The reason probably lies in that the extra Li ions in the TM layer might behave as in $LiNi_{0.5}Mn_{0.5}O_2$ forming tetrahedral dumbbells upon Li removal.[22] In addition, as the Li content in the compound increases, more Ni^{2+} ions are oxidized to Ni^{3+} further reducing the electrochemical capacity. However, at lower current densities and at elevated temperatures, the excess lithium ions do result in higher capacities.[24]

Advanced Magnetic Characterization. We showed earlier that the determination of transition metal oxidation states through the magnetic properties could be used to determine the stoichiometry of the layered oxides beyond the sensitivity of powder XRD and DCP analysis. It has long been established that the magnetic properties of these layered oxides are sensitive to the extent of Li/Ni disorder (see ref. [9] and references therein), which we have observed for the $Li_{1+z}(Ni_{0.45}Mn_{0.45}Co_{0.1})_{1-z}O_2$ series. However, the $LiNi_{0.45}Mn_{0.45}Co_{0.1}O_2$ series synthesized at various temperatures show similar trend in magnetic properties (compare Figure 2 and Figure 10), while the amount of Ni_{Li} is this series does not change significantly. Our previous studies of $Li_xNi_{0.5}Mn_{0.5}O_2$ magnetism has indicated that magnetic ordering within the TM layers should be considered along with interlayer ordering mediated by the Ni_{Li} ions. Using AC and DC magnetic susceptibility data we have shown that the magnetic order in this compound is established within finite-size clusters through a series of magnetic transitions. At 90 K Ni^{2+} spins of Ni_{Li} and Ni_{TM} connected by 180° Ni−O−Ni bond order forming magnetic clusters propagating in *c* direction. This is accompanied by a DC susceptibility increase and a strong peak of imaginary component of the AC susceptibility. Between 60 and 40 K, Mn^{4+} spins connected to Ni_{TM} spins by 90° Ni−O−Mn exchange order, which induces the growth of magnetic clusters within the layers. In this temperature interval, major increase of the DC susceptibility occurs, while $\chi''(T)$ shows a second maximum. We have noticed that temperature dependences of the DC susceptibility measured under ZFC conditions shows maxima at the same temperatures as $\chi''(T)$. Here we further develop the model of the magnetic interactions based on analysis of ZFC susceptibilities of $Li_{1+z}(Ni_{0.45}Mn_{0.45}Co_{0.1})_{1-z}O_2$ compounds. Our ultimate goal is to establish structure-magnetic properties relations allowing use of magnetism as a signature of TM ordering.

As was established earlier, at high temperatures, all the compounds are Curie−Weiss paramagnets. At lower temperatures a deviation from the Curie−Weiss law is observed for all the investigated materials, namely, an increase in magnetic susceptibility, the magnitude and temperature of which depends strongly on the composition. The susceptibilities measured under FC and ZFC conditions deviate below a certain temperature, which is designated as blocking temperature T_b (Figure 16). For the materials with high Li content ($z + 1 = 1.2$ and 1.1) the blocking temperatures are low, 7.0 and 7.5 K, respectively (Figure 16 and Table 3). ZFC susceptibilities show a cusp below T_b, which is typical of a spin-glass transition. In these compounds Ni_{Li} content is below 2%, and the TM layers are diluted with nonmagnetic Li^+ and Co^{3+} ions, therefore large-size magnetic clusters cannot be formed and a spin-glass state is developed. A spin-glass state was found previously in $LiNi_{0.4}Mn_{0.4}Co_{0.2}O_2$.[9]

In the stoichiometric $LiNi_{0.45}Mn_{0.45}Co_{0.1}O_2$ the FC and ZFC curves depart at much higher temperature of 65 K. Below

(19) Delmas, C.; Peres, J. P.; Rougier, A.; Demougues, A.; Weill, F.; Chadwick, A.; Broussely, M.; Perton, F.; Biensan, P.; Willmann, P. *J. Power Sources* **1997**, *68*, 120.
(20) Whittingham, M. S.; Gamble, F. R. *Mater. Res. Bull.* **1981**, *16*, 37.
(21) Makimura, Y.; Ohzuku, T. *J. Power Sources* **2003**, *119−121*, 156.
(22) Breger, J.; Meng, Y. S.; Hinuma, Y.; Kumar, S.; Kang, K.; Shao-Horn, Y.; Ceder, G.; Grey, C. P. *Chem. Mater.* **2006**, *18*, 4768.
(23) Van der Ven, A.; Ceder, G. *Electrochem. Commun.* **2004**, *6*, 1045.
(24) Johnson, C. S.; Li, N.; Lefief, C.; Thackeray, M. M. *Electrochem. Commun.* **2007**, *9*, 787.

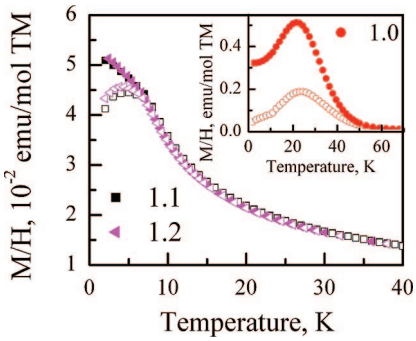

Figure 16. Temperature dependences of magnetic susceptibility of $Li_{1+z}(Ni_{0.45}Mn_{0.45}Co_{0.1})_{1-z}O_2$ measured under field-cooling (solid symbols) and zero-field-cooling (open symbols) conditions. The label indicates Li content $1 + z$.

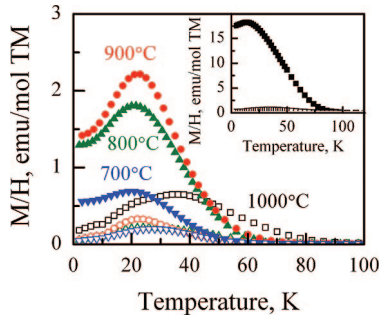

Figure 17. Temperature dependences of magnetic susceptibility of $LiNi_{0.45}Mn_{0.45}Co_{0.1}O_2$ synthesized at various temperatures measured under field-cooling (solid symbols) and zero-field-cooling (open symbols) conditions. The inset shows FC and ZFC data for 1000 °C sample.

this temperature, both curves show broad maxima centered at about 22 K; in addition, the ZFC curve shows a pronounced change of slope at 10 K. FC and ZFC curves of $LiNi_{0.45}Mn_{0.45}Co_{0.1}O_2$ samples synthesized at various temperatures are shown in Figure 17. With synthesis temperature increase, the blocking temperature and the magnitude of susceptibility maxima increase. This increase is relatively small between 700, 800, and 900 °C samples, whereas the 1000 °C sample is essentially different. The blocking temperature is as high as 160 K in this sample and the FC susceptibility increase observed below 100 K is five times stronger than that of 800 °C sample.

With decrease in Li content, the magnetic properties change significantly as a result of the increase in the magnetic ion concentration and spin number (Figure 18). At $1 + z = 0.9$ (lithium content is 0.9), a strong increase in the magnetic susceptibility is found at about 150 K, FC and ZFC curves depart noticeably below 165 K. At $1 + z = 0.8$, an additional change in slope is observed for both FC and ZFC curves at around 90 K. This is consistent with the progressive formation of a spinel phase observed in the X-ray diffraction data. Finally, at $1 + z = 0.5$, two magnetic transitions are observed: the transition at 90 K is accompanied by the susceptibility increase, whereas at 30 K, the susceptibility decreases (Figure 18). Such behavior may be attributed to a reentrant transition known in spinels. Upon a temperature decrease, a magnetically ordered phase is formed first, which is most likely to be ferrimagnetic in our case. However, upon

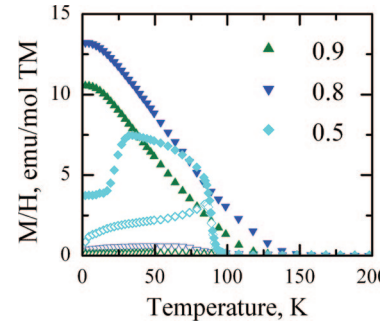

Figure 18. Temperature dependences of magnetic susceptibility of $Li_{1+z}(Ni_{0.45}Mn_{0.45}Co_{0.1})_{1-z}O_2$ measured under field-cooling (solid symbols) and zero-field-cooling (open symbols) conditions. The label indicates Li content $1 + z$.

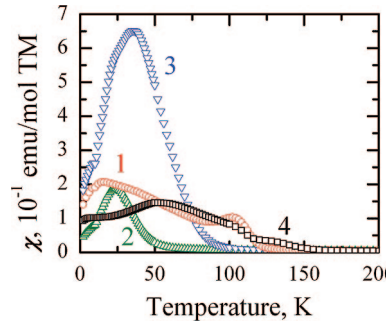

Figure 19. Zero-field-cooled susceptibilities as a function of temperature for (1) $LiNi_{0.5}Mn_{0.5}O_2$, (2) $LiNi_{0.45}Mn_{0.45}Co_{0.1}O_2$ synthesized at 800 °C, (3) $LiNi_{0.45}Mn_{0.45}Co_{0.1}O_2$ synthesized at 1000 °C, and (4) $Li_{0.9}(Ni_{0.45}Mn_{0.45}Co_{0.1})_{1.1}O_2$.

further temperature decrease, this phase becomes unstable and the system reenters a glassy state.[25]

It is interesting to compare the ZFC curves of $LiNi_{0.45}Mn_{0.45}Co_{0.1}O_2$ (800 and 1000 °C samples) and $Li_{0.9}(Ni_{0.45}Mn_{0.45}Co_{0.1})_{1.1}O_2$ against the base case of $LiNi_{0.5}Mn_{0.5}O_2$ (Figure 19). This comparison immediately reveals that the $LiNi_{0.45}Mn_{0.45}Co_{0.1}O_2$ samples do not show the maximum corresponding to the $Ni^{2+}-Ni^{2+}$ 180° magnetic cluster ordering; only intralayer magnetic cluster ordering is revealed by the ZFC curves. In contrast, $Li_{0.9}(Ni_{0.45}Mn_{0.45}Co_{0.1})_{1.1}O_2$ shows a double-step transition with susceptibility increase around 110 and 150 K, which corresponds to 180° cluster formation, similar to that observed in $LiNi_{0.5}Mn_{0.5}O_2$. According to the Rietveld refinement data, the $1 + z = 0.9$ sample has about 9% Ni^{2+} ions in the Li layer, essentially the same as in $LiNi_{0.5}Mn_{0.5}O_2$, whereas in $LiNi_{0.45}Mn_{0.45}Co_{0.1}O_2$, the Ni_{Li} content is around 6%. The most significant difference between these samples is not the amount of Ni in the Li layer, but the amount of nonmagnetic ions, such as Li^+ and Co^{3+} in the TM layer, which decreases from 16% in $LiNi_{0.45}Mn_{0.45}Co_{0.1}O_2$ to 8% in $LiNi_{0.5}Mn_{0.5}O_2$ to 0% in $Li_{0.9}(Ni_{0.45}Mn_{0.45}Co_{0.1})_{1.1}O_2$. These nonmagnetic ions effectively terminate the propagation of 180° bound clusters in the *c*-direction as these clusters are essentially one-dimensional double chains only weakly correlated between each other in the absence of intralayer ordering. Thus, the increase in the transition temperature for

(25) Muraleedharan, K.; Srivastava, J. K.; Marathe, V. R.; Vijayaraghavan, R. *J. Phys. C: Solid State Phys.* **1985**, *18*, 5355.

$Li_{0.9}(Ni_{0.45}Mn_{0.45}Co_{0.1})_{1.1}O_2$ can be attributed to the increase of 180°-bound cluster sizes. The two-step nature of this transition suggests that along with familiar 180° $Ni^{2+}-Ni^{2+}$ interactions, another strong 180° exchange, such as $Ni^{2+}-Mn^{3+}$, may be involved.

The ordering of the intralayer clusters occurs at a lower temperature than that of the interlayer clusters because the 90° magnetic exchange is weaker than the 180° one. The temperature of intralayer ordering depends strongly upon the amount of nonmagnetic ions in the layer. For example, intralayer clusters in $Li_{0.9}(Ni_{0.45}Mn_{0.45}Co_{0.1})_{1.1}O_2$ order at higher temperature than in $LiNi_{0.5}Mn_{0.5}O_2$ as all the TM ions in this compound are magnetic and the clusters can grow bigger in the nondiluted layers. A similar effect is observed in the 1000 °C $LiNi_{0.45}Mn_{0.45}Co_{0.1}O_2$ sample, where ZFC maximum shifts toward higher temperatures as compared to 800 °C sample. As we have established earlier the 1000 °C sample is lithium deficient as in $Li_{1+z}M_{1-z}O_2$ ($1 + z < 1$). The combination of DCP, Rietveld refinement, and magnetic properties gives the formula $[Li_{0.942}Ni_{0.058}{}^{2+}]-[Ni_{0.048}{}^{2+}Mn_{0.466}{}^{4+}Co_{0.069}{}^{2+}Co_{0.035}{}^{3+}Li_{0.022}]O_2$ meaning that the concentration of nonmagnetic ions in the TM layer drops to 5.7% in 1000 °C compared to 16% in 800 °C sample. It is interesting to note that the low-temperature magnetization observed in this sample is the highest of all materials considered in this paper. Possible reason might be the large particle size attained at 1000 °C synthesis. Larger particle and crystallite size would allow formation of larger magnetic clusters or domains producing stronger net magnetization.

Summarizing the magnetic studies, magnetic properties were the key technique for understanding the effect of synthesis temperature on the structure and stoichiometry of $LiNi_{0.45}Mn_{0.45}Co_{0.1}O_2$. It allowed the determination of the transition metal oxidation states and, combined with DCP and Rietveld refinement, to suggest the chemical composition and distribution of metal ions in the layered structure, which was further confirmed by FC-ZFC susceptibilities studies. We were able to correspond the peaks observed in the temperature dependences of the ZFC susceptibility to the ordering of intralayer and interlayer magnetic clusters. The temperature of these peaks as well as the magnitude of the low-temperature magnetization and the size of the hysteresis loop depends upon three major factors: (1) the concentration of Ni^{2+} in the Li layer, (2) the degree of nonmagnetic dilution of the TM layers, and (3) the crystallite size. This model allows to rationalize magnetic properties of all $Li_{1+z}(Ni_yMn_zCo_{1-y-z})_{1-z}O_2$ samples synthesized in our group. The next step will be confirmation of this model by studying local magnetism using neutron scattering and μSR as well as the development of quantitative models.

Conclusion

The processing-structure-property relations in $Li_{1+z}(Ni_{0.45}Mn_{0.45}Co_{0.1})_{1-z}O_2$, a low-cobalt -content cathode material for Li-ion batteries, have been investigated. The synthesis temperature has a pronounced effect on the electrochemical properties of the materials as both particle size and the stoichiometry are affected. The 800 °C synthesis temperature provides the desired stoichiometry if 5% excess Li is used, well-developed layered structure, and optimum particle size, which results in excellent electrochemical behavior (~180 mAh/g at 0.5 $mAcm^2$ between 2.5 and 4.6 V), with the actual capacity depending on the charging voltage. Lower synthesis temperature gives somewhat under-reacted product, which is lithium-deficient with incomplete layered structure. Higher-synthesis-temperature products have excellent layered structure and good crystallinity; however, Li content $1 + z$ tends to get lower than the targeted value, and particle size gets too large, resulting in quick capacity fading upon cycling. Synthesis temperature and cooling method have little or no influence on the amount of Ni in the Li layer, whereas the lithium content does. The Rietveld refinement of the X-ray diffraction data has shown a decrease of cation disorder between Ni^{2+} and Li^+ with increasing lithium content. This point is further confirmed by the appearance of the magnetization hysterysis loops when lithium content is as low as 0.8 or 0.9. The lithium-deficient $Li_{0.9}[Ni_{0.45}Mn_{0.45}Co_{0.1}]_{1.1}O_2$ compound shows the best electrochemical properties in the series because of the absence of Li in the transition metal layer and the stabilization the layered structure through interlayer Ni^{2+}. Extra amount of lithium does not help to improve the electrochemical properties since this lithium residing in the TM layer drops to the tetrahedral sites in the Li layer during the charge and becomes hard to be removed within the normal voltage range. Only when a slight excess amount of lithium is added (Li/TM = 1.05) is the first discharge capacity improved compared to the stoichiometric compound (194 mAh/g at 0.1 mA/cm^2 between 2.5 and 4.6 V). This might be attributed to the slight reduction of Ni content in the Li layer, which facilitates lithium diffusion. Compared with $LiNi_{0.4}Mn_{0.4}Co_{0.2}O_2$, $LiNi_{0.45}Mn_{0.45}Co_{0.1}O_2$ delivers close discharge capacity of about 180 mAh/g in the first cycle with slightly higher charge−discharge plateau. However, smaller polarization was observed for $LiNi_{0.4}Mn_{0.4}Co_{0.2}O_2$ than that of $LiNi_{0.45}Mn_{0.45}Co_{0.1}O_2$. Both $LiNi_{0.45}Mn_{0.45}Co_{0.1}O_2$ and $LiNi_{0.4}Mn_{0.4}Co_{0.2}O_2$ could deliver as high capacities as reported for $LiNi_{1/3}Mn_{1/3}Co_{1/3}O_2$ with even more stable cycling performance. The rational choice among stoichiometric compounds in this system should be either $LiNi_{0.40}Mn_{0.40}Co_{0.2}O_2$ or $LiNi_{0.45}Mn_{0.45}Co_{0.1}O_2$ depending on the actual needs. When a significant amount of Li occurs in the transition metal layer at low Co contents, Li deficient compounds are a good choice. The extent of lithium deficiency should be tailored to minimize Li content in the transition metal layer as in $Li_{0.9}(Ni_{0.45}Mn_{0.45}Co_{0.1})_{1.1}O_2$.

Acknowledgment. We thank the U.S. Department of Energy, Office of FreedomCAR and Vehicle Technologies, for financial support through the BATT program at Lawrence Berkeley National Laboratory. Financial support from the National Science Foundation, DMR 0705657, is also greatly appreciated.

CM802316D